Free-carrier contribution to the optical response of N-rich Cu_3N thin films

2009 J. Phys. D: Appl. Phys. 42 165101

(http://iopscience.iop.org/0022-3727/42/16/165101)

IOP PUBLISHING JOURNAL OF PHYSICS D: APPLIED PHYSICS

J. Phys. D: Appl. Phys. **42** (2009) 165101 (6pp) doi:10.1088/0022-3727/42/16/165101

Free-carrier contribution to the optical response of N-rich Cu_3N thin films

N Gordillo[1], R Gonzalez-Arrabal[2], A Álvarez-Herrero[3] and F Agulló-López[1,4]

[1] Centro de Microanálisis de Materiales, Universidad Autónoma de Madrid 28049-Madrid, Spain
[2] Instituto de Microelectrónica de Madrid CSIC C/ Isaac Newton, 8. Tres Cantos, 28760-Madrid, Spain
[3] Laboratorio de Instrumentación Espacial, INTA, Torrejón de Ardoz, 28850-Madrid, Spain
[4] Departamento de Física de Materiales, Universidad Autónoma de Madrid 28049-Madrid, Spain

E-mail: nuria.gordillo@uam.es

Received 20 December 2008, in final form 5 May 2009
Published 23 July 2009
Online at stacks.iop.org/JPhysD/42/165101

Abstract

The influence of nitrogen excess on the optical response of N-rich Cu_3N films is reported. The optical spectra measured in the wavelength range from 0.30 to 20.00 μm have been correlated with the elemental film composition which can be adjusted in the nitrogen atomic percentage (at%) range from 27 ± 2 up to 33 ± 2. The absorption spectra for the N-rich films are consistent with direct optical transitions corresponding to the stoichiometric semiconductor Cu_3N plus a free-carrier contribution that can be tuned in accordance with the N-excess. The data are consistent with the incorporation of the excess N in the lattice as an electron acceptor that generates free holes.

1. Introduction

Cu_3N has been suggested as an interesting material for a number of nano-electronic and nano-photonic devices, such as spin tunnel junctions [1] and high density optical storage media [2, 3]. Different methods have been applied to grow films with reasonable quality: molecular beam epitaxy [4], atomic layer deposition [5], pulsed laser deposition [6], dc triode sputtering [7] and, mostly, RF magnetron sputtering [8–11]. Cu_3N films present a cubic anti-ReO_3 type crystal structure [12], which is quite suited for the incorporation of other elements such as Pd in the body-centre position of the cubic unit cell, and form ternary compounds [13, 14].

As for other metal nitrides [15–17], the chemical composition of the films which varies from Cu- to N-rich, notably depends on the deposition conditions and can be tuned by changing them. Technological implementation of Cu_3N-based devices requires reproducible physical properties and therefore samples with a well-defined stoichiometry. Unfortunately, up to now, in most works the stoichiometry has been poorly characterized, being mainly deduced from XRD data (changes in the lattice parameter) or even not measured. This is probably due to the difficulty in performing a reliable stoichiometry characterization in these kinds of compounds because of their metastability and low decomposition temperature. This lack of knowledge of the real stoichiometry of the films has led to large discrepancies in the reported values for many relevant physical properties. This is, indeed, a relevant drawback for industrial implementation of the material. As an example, the reported electrical conductivity ranges from above $10^3\ \Omega^{-1}\,cm^{-1}$ (quasi-metallic behaviour [4–10]) to $10^{-3}\ \Omega^{-1}\,cm^{-1}$ (semiconducting behaviour [18–22]). On the other hand, although most optical absorption data indicate that the material is semiconducting with a forbidden gap around or above 1 eV, the reported values spread over a wide range (0.9–1.9 eV) [23–25].

Contactless optical techniques have been demonstrated to be a powerful method to know about the electronic structure of the valence and conduction bands as well as on defect and impurity levels in epilayers or multilayer semiconducting systems. The use of those techniques for nitrides characterization allows overcoming the well known difficulties for fabricating low resistance ohmic contacts on these kinds of materials [26–28]. Moreover, most of the methods employed for the fabrication of suitable contacts involve annealing steps, which are critical in the particular case of metastable nitrides since they thermally decompose at relatively low temperatures [29, 30]. The information provided by contactless optical methods is in a way comparable to that

derived from UV and x-ray photoemission spectra [4]. The wavelength restriction in the optical studies performed so far in Cu_3N layers, has hindered up to now the achievement of reliable conclusions.

This work focuses on the study of the optical properties of copper nitride films with atomic percentages of nitrogen ranging from 27 ± 2 to 33 ± 2 as determined by the ion beam analysis (IBA) techniques. They offer a unique tool to determine the film composition and, for RBS, provide an absolute calibration. Optical measurements have been now performed in a wider wavelength range (from 0.30 to 20.00 μm) than that reported in previous work [25]. The optical data are consistent with direct band-to-band transitions together with a free-carrier contribution, not detected so far, that clearly increases with nitrogen contents. The data are discussed in terms of the formation of electron acceptor centres associated to interstitial nitrogen excess.

2. Experimental

Copper nitride thin films of ∼80 nm thickness with an atomic nitrogen concentration ranging from 27 to 33 at% were deposited by dc triode sputtering from a commercial copper target on Si (1 0 0) single crystals in the presence of an Ar + N atmosphere at a cathode voltage (dc bias) of −0.5 kV. This cathode voltage value has been demonstrated to allow a large range of nitrogen contents in the films and to achieve more crystalline samples than those deposited at higher cathode voltage. For more information see [7]. The total gas pressure ($P_{Ar} + P_{N_2}$) and the target–substrate distance were kept constant at 8×10^{-3} mbar and 8 cm, respectively, whereas the nitrogen partial pressure was varied from 20% to 100%.

The film thickness has been measured by profilometry and further corroborated by ellipsometry. For profilometry measurements, films were partially covered with a mask during deposition.

IBA techniques, in particular Rutherford and non-Rutherford backscattering spectroscopy (RBS, non-RBS) in combination with nuclear reaction analysis (NRA), were used to determine the elemental composition of the films. The RBS and non-RBS measurements were performed at the Centre of Microanalysis of Materials (CMAM/UAM) [31, 32] using a He^+ beam at the energy of 2.0 MeV and 3.7 MeV, respectively. The NRA measurements were carried out at the Institute of Ion Beam Physics and Materials Research in Forschungszentrum Dresden-Rossendorf (FZD) using a D^+ beam at the energy of 1.8 MeV and the nuclear reaction $^{14}N(d,\alpha)^{12}C$ [33]. Special care was taken to ensure that the chemical composition of the samples was not affected by the analysis conditions. Four IBA spectra were sequentially measured in the same spot and under the same conditions and at a fluence higher than the one used for the standard analysis in order to assure that the elemental chemical composition of the samples does not change neither by He^+ nor by D^+ irradiation. The beam current densities were kept very low to avoid any significant heating of the samples.

A more complete picture about deposition conditions and nitrogen contents determination can be found in [7, 34].

Table 1. Brief overview of deposition parameters and properties of the six studied samples. In this table, P_{Ar}/P_{N_2} accounts for the ratio between the argon and the nitrogen pressures during sputtering, dc bias stands for the cathode voltage, [N] refers to the atomic percentage of nitrogen and a is the lattice parameter. The thickness values measured by profilometry are presented in the fifth column whereas the sixth column yields those giving the best fit for SE data.

P_{Ar}/P_{N_2}	DC_{bias} (kV)	[N] (at%)	a (Å)	Thickness (nm) profilometry	Thickness (nm) SE
0.2	−0.5	27 ± 2	3.8621	78 ± 3	76 ± 1
0.3	−0.5	29 ± 2	3.8692	82 ± 3	77 ± 1
0.4	−0.5	30 ± 2	3.8752	78 ± 3	75 ± 1
0.6	−0.5	32 ± 2	3.8782	76 ± 3	79 ± 1
0.9	−0.5	33 ± 2	3.8679	82 ± 3	79 ± 1
1.0	−0.5	33 ± 2	3.8655	65 ± 3	65 ± 1

The structural characterization was done *ex situ* by x-ray diffraction (XRD) using a Philips X'Pert four cycle diffractometer with a Cu K_α radiation source in the Bragg–Brentano geometry.

The optical characterization of the films was carried out in two different set-ups for the visible and infrared ranges. From 0.30 to 1.80 μm spectra have been recorded with a J A Woollam Co. [35] ellipsometer at the incident angles of 65° and 70° for the complex refractive index determination, whereas for the range 1.40–20.00 μm a Fourier transform IR spectrophotometer (FT-IR Bruker IFS60v) was used. All optical measurements in this work were carried out at room temperature.

3. Results

The chemical and physical properties of six copper nitride thin films were characterized. The atomic percentage of nitrogen (N at%) in the samples was determined by the combination of RBS, non-RBS and NRA techniques to be 27 ± 2 (one sample), 30 ± 2 (two samples) and 33 ± 2 (three samples). A brief description of the deposition conditions and of the characteristic of the films is given in table 1.

According to the XRD data all samples are polycrystalline and preferentially oriented along the (1 0 0) crystallographic axes [7]. As shown in table 1, small variations in the lattice parameter, of the order of 1%, are observed for films with diverse stoichiometry deposited at different P_{Ar}/P_{N_2} ratios. These results contrast somehow with those previously published by Hou [36] who theoretically predicts a clear dependence of the lattice parameter on stoichiometry and nitrogen location within the films. Nevertheless, the calculations by Hou cannot be directly compared with our experimental XRD data since the experimental lattice parameter for films sputtered under different conditions is indeed determined by a convolution of two diverse effects: (i) the nitrogen contents and its location within the film and (ii) the known changes in the stress state of the sputtered films due to the differences in the deposition parameters [37, 38].

The spectroscopic ellipsometry (SE) parameters Ψ and Δ, measured in the 0.30–1.80 μm range at an incidence angle of

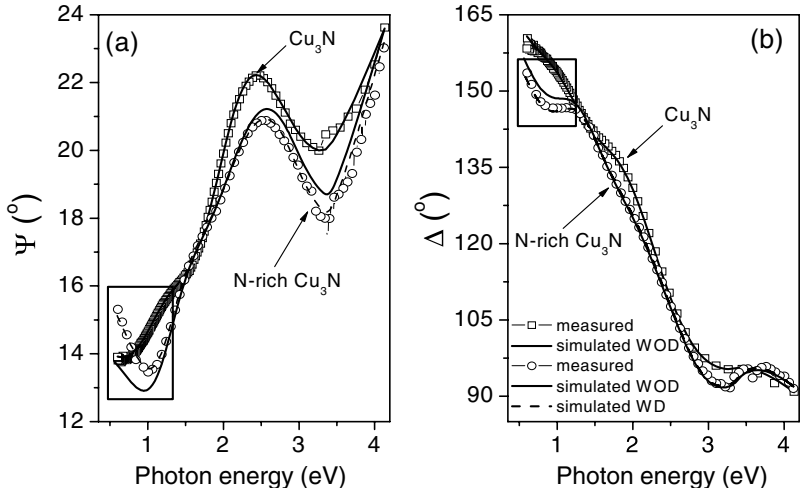

Figure 1. Measured SE parameters Ψ (*a*) and Δ (*b*) for a nearly stoichiometric (open squares) and for a N-rich (open circles) Cu_3N layer. Simulated SE considering a Drude component, WD (dash black line), and without considering it, WOD (black line), are also displayed for these two layers. For clarity, the spectra are only depicted at an angle of incidence of 65°.

Table 2. Atomic percentage of nitrogen [N], average Drude parameters and optical gap energy for the six studied films. In this table, ω_p is the plasma frequency, N the density of free carries and γ is the carrier dissipation factor. The values represent an average over the number of layers indicated in the table.

Number of investigated layers	[N] at%	ω_p (Hz)	N (cm^{-3})	γ (Hz)	E_G (eV)
1	27	—	—	—	1.07
2	30	$(1.0 \pm 0.1) \times 10^{14}$	$(3.2 \pm 0.9) \times 10^{18}$	$(1.1 \pm 0.3) \times 10^{14}$	1.13
3	33	$(2.1 \pm 0.1) \times 10^{14}$	$(1.4 \pm 0.1) \times 10^{19}$	$(1.45 \pm 0.02) \times 0^{14}$	1.25

65° are shown in figures 1(*a*) and (*b*), respectively, for films having a nitrogen contents of 27 ± 2 at% (referred from now on as stoichiometric Cu_3N) and 33 ± 2 at% (referred as N-rich Cu_3N). Other films with intermediate nitrogen contents have also been investigated but they are not included in the figure for clarity sake. The data have been analysed within a three-layer model consisting of air (layer 1), the Cu_3N film with thickness d (layer 2) and the high reflectivity Si substrate (layer 3). As illustrated in figure 1 the two SE spectra can be well fitted, in the high-energy region (>1.3 eV), by assuming three Gaussian bands. However, to achieve a good fit for the low-energy part (below ∼1.3 eV) in the case of N-rich layers it is necessary to add a Drude (free-carrier) component [39], described by the following expression:

$$\tilde{n}^2 = -\frac{\omega_p^2}{\omega^2 + i\gamma\omega} = -\frac{\omega_p^2}{\omega^2 + \gamma^2} + i\frac{\omega_p^2\gamma}{\omega^3 + \gamma^2\omega}, \qquad (1)$$

where ω_p is the plasma frequency, $\omega_p = (Ne^2/\varepsilon_0 m^*)^{1/2}$, γ the dissipation factor in the free-carrier dynamics, N the density of free carriers and m^* the effective carrier mass. The values obtained for these parameters from the fitting to the SE spectra are listed in table 2 for three representative compositions investigated in this work. Each set of parameters represents an average over the number of samples indicated in the table. From these data it is observed that the plasma frequency increases with the nitrogen contents. The carrier density N, given as an illustrative value, has been determined assuming that m^* is equal to the free electron mass.

The dispersion curves for the refractive index (n) and extinction coefficients (κ) derived from the fits in figure 1 are shown in figures 2(*a*) and in (*b*), respectively. The absorption coefficient, $\alpha = 2k\omega/c$, represented in figure 3, reaches high values (∼10^5 cm^{-1}) in the visible range in accordance with the direct optical transitions between the valence and conduction bands. Moreover, it shows two main components peaked at around 2 and 4 eV in reasonable agreement with the UV photoemission measurements and closely related to the density of states for the valence band [4]. A closer view reveals that an increasing absorption develops for photon energies below 1 eV for the N-rich Cu_3N films in accordance with the presence of a free-carrier (Drude) contribution. This contribution clearly influences the determination of the direct energy gap, E_G, of the semiconductor within the parabolic approximation, $\alpha(h\nu) = A(h\nu - E_G)^{1/2}$, and should be removed to perform a reliable extrapolation to the E_G value. As illustrated in the inset of figure 3, the value of the gap obtained by extrapolation to $\alpha = 0$ in an α^2 versus $h\nu$ plot is quite sensitive to the presence of a Drude contribution. It clearly increases from 1.07 eV for the stoichiometric sample to 1.25 eV for the N-rich one in accordance with the hole-filling effect in the valence band [39]. This correction is relevant and, to our knowledge, it has not been considered in previous determinations of E_G for copper nitrides.

In order to more clearly reveal the Drude component, Fourier transform infrared spectroscopy (FTIR) was used to measure the reflectance spectra in the range from 1.40 to 20.00 μm. FTIR data are shown in figure 4 for the samples

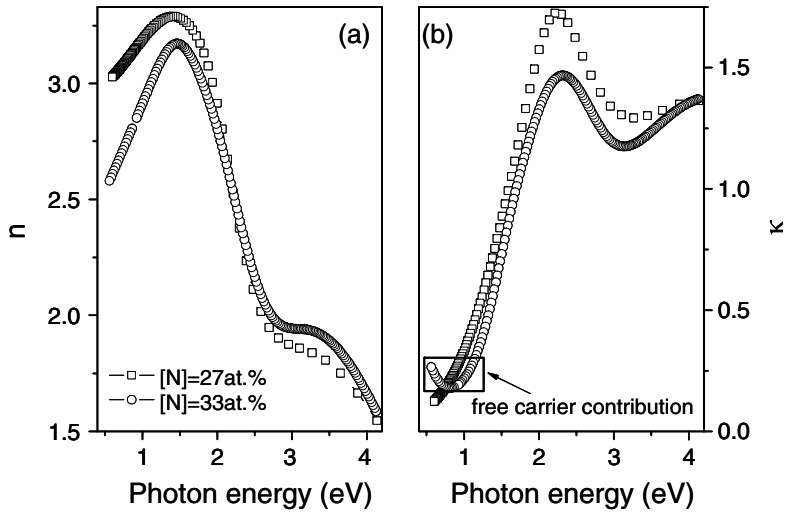

Figure 2. Dispersion curves for the refractive index n (a) and extinction coefficient κ (b) for a stoichiometric (open squares) and for a N-rich (open circles) Cu_3N layer. The dark square indicates the free-carrier contribution to κ.

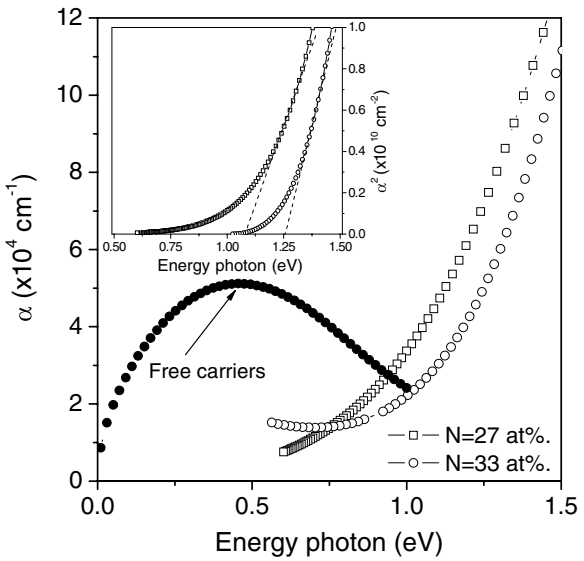

Figure 3. Absorption coefficient (α) as a function of wavelength for a stoichiometric (open squares) and for a N-rich (open circles) Cu_3N film. The filled circle indicates the free carrier contribution. The inset shows the determination of the gap energy for the two films within the parabolic approximation. Note that higher gap energy is obtained for the N-rich film.

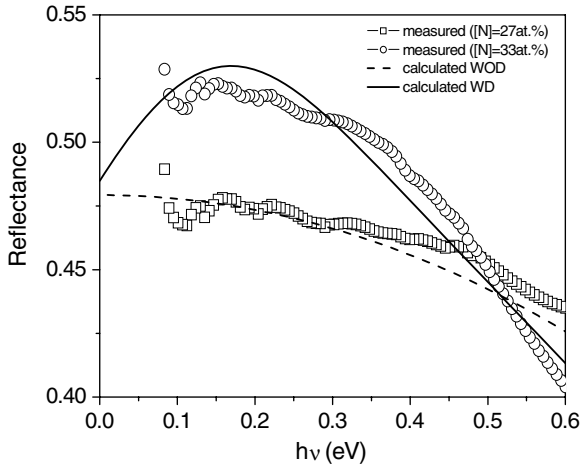

Figure 4. Measured reflectance spectra for a stoichiometric (open squares) and for a N-rich (open circles) Cu_3N layer. Calculated reflectance spectra assuming the three-layer model without considering any Drude component, WOD (dash black line) and considering it, WD (black line).

with the extreme N contents used in this study. The main observed effect is an overall rise in the reflectance and a more pronounced increase at the lower photon energies for the N-rich sample. To quantitatively analyse the spectral dependence we have used, again, the three-layer model that leads to the following expression for the reflectance (R):

$$R = \left| \frac{r_{12} + r_{23} e^{i\delta}}{1 + r_{12} r_{23} e^{i\delta}} \right|^2, \qquad (2)$$

where r_{12} and r_{23} correspond to the complex amplitude reflectivities for the 1–2, and 2–3 interfaces,respectively. The phase change for every return light path in the film is $\delta = 4\pi d n_2 \cos\theta_2/\lambda$, θ_2 corresponding to the inclination of the wavevector with respect to the normal to the Cu_3N film (medium 2). The calculated spectral reflectances, either including (WD) or not (WOD) the Drude contribution, are respectively shown in figure 4. Calculations assume wavelength-independent refractive indices for the semiconductor contribution to the film as well as, for the silicon substrate. The outcome indicates a good agreement between the calculated and the experimental spectra. From these results, it is clear that the Drude contribution explains the main trends observed from the experimental data.

4. Discussion

The stoichiometric sample behaves as an intrinsic semiconductor, whereas a strong free carrier contribution is observed for non-stoichiometric films. In principle, from the IBA measurements it cannot be distinguished whether the deviations from the Cu_3N stoichiometry are due to the

presence of extra nitrogen (nitrogen interstitials) or to a deficit of copper (copper vacancies) in the samples. However, from previous experiments on similar metal nitrides it is known that nitrogen incorporates into the compounds as interstitials [15]. Moreover, taking into account that the copper sublattice is more stable than that for nitrogen as suggested by the thermal and radiation-induced decomposition of the material experiments [2, 3, 10] and the information gathered in this paper we may consider that the free carriers are, indeed, holes. As a reasonable scheme we, here, propose that a substantial fraction of nitrogen atoms (possibly as N^0) has incorporated at some interstitial sites in the open structure and act as electron acceptor centres. The body-centre position of the cubic unit cell is the natural candidate since it has been shown that a number of impurity ions, such as Pd, can occupy this position [13, 14]. Moreover, the good agreement of the optical data with the Drude model permits to rule out other possible mechanisms for the observed spectra (indirect intrinsic transitions or transitions to or from intermediate defect levels in the band gap).

The presence of a free-hole concentration at the top of the valence band should also have relevant implications on the analysis of the optical spectra. In particular, it should lower the Fermi level and induce a corresponding increase in the energy of the lowest allowed direct transition. This effect that implies an apparent increase in the energy gap of the semiconductor is, indeed, observed in our data (see table 2).

Anyhow, one cannot rule out that the interstitial lattice position of the excess nitrogen may compete with its trapping at extended defects like grain boundaries. The investigation of the nitrogen location in the Cu_3N films is a relevant topic that should be further pursued.

It is worthwhile to mention here that our results contrast somehow with those reported by Yue *et al* [12, 40] using Hall measurements, suggesting that the Cu_3N shows an n-type semiconductor behaviour. In our opinion the divergences found in the behaviour of the material should be explained in terms of difference in film stoichiometry. Indeed, in Yue's publications the elemental composition of the films was not determined; instead it has been deduced from the XRD data in combination with the growth parameters (changes in the nitrogen flow rate). However, a previous publication [7] demonstrates that the relation between nitrogen incorporation into the films and growth parameters is not linear at all.

5. Summary and conclusions

In summary, the optical properties of polycrystalline N-rich Cu_3N films are consistent with the behaviour expected for an intrinsic semiconductor (corresponding to the stoichiometric Cu_3N) together with a variable free-carrier contribution that is correlated with the nitrogen excess. This contribution becomes observable for wavelengths above around 1 μm and is responsible for an increase in the measured direct optical gap as well as for some reflectivity changes in the IR. The Drude contribution suggests that the nitrogen excess is incorporated in the lattice as an electron acceptor centre. Therefore, we have shown that stoichiometry plays a significant role in the optical response of the material and offers a way to tune the gap of the semiconductor, which may be attractive for the electronic-device industry.

Acknowledgments

The authors thank Dr Olivares-Villegas for his invaluable help and Dr Wagner for helpful discussions. The authors acknowledge the M.E.C. and C.S.I.C. for the Juan de la Cierva (R.G.A) and M.C.Y.T (Grant MAT2005-03011) (N.G.G) for the financial support. NRA measurements were supported by the EU-Research Infrastructures Transnational Access Programme at the AIM Centre for Application of Ion Beams in Materials Research under EC contract No. 025646.

References

[1] Borsa D M, Grachev S and Boerma D O 2002 *IEEE Trans. Magn.* **38** 2709
[2] Asano M, Umeda K and Tasaki A 1990 *Japan. J. Appl. Phys.* **29** 1985
[3] Maruyama T and Morishita T 1996 *Appl. Phys. Lett.* **69** 890
[4] Navio C, Capitán M J, Álvarez J, Yndurain F and Miranda R 2007 *Phys. Rev.* B **76** 085105
[5] Törndahl T 2004 *PhD Thesis* ISBN 91-554-6081-X
[6] Gallardo-Vega C and de la Cruz W 2006 *Appl. Surf. Sci.* **252** 8001
[7] Gordillo N, Gonzalez-Arrabal R, Martin-Gonzalez M S, Olivares J, Rivera A, Briones F, Agulló-López F and Boerma D O 2008 *J. Cryst. Growth* **310** 4362
[8] Maruyama T and Morishita T 1995 *J. Appl. Phys.* **78** 4104
[9] Kim K J, Kim J H and Kang J H 2000 *J. Cryst. Growth* **222** 767
[10] Nosaka T, Yoshitake M, Okamoto A, Ogawa S and Nakayama Y 2001 *Appl. Surf. Sci.* **169** 358
[11] Du Y, Ji A L, Ma L B, Wang Y Q and Cao Z X 2005 *J. Cryst. Growth* **280** 490
[12] Yue G H, Yan P X, Liu J Z, Wang M X, Li M and Yuan X M 2005 *J. Appl. Phys.* **98** 103506
[13] Du Y, Huang R, Song R, Ma L B, Liu C, Li C R and Cao Z X 2007 *J. Mater. Res.* **22** 3052
[14] Fan X, Wu Z, Li H., Geng B, Li C and Yan P 2007 *J. Phys. D: Appl. Phys.* **40** 3430
[15] Coey J M D and Smith P A I 1999 *J. Magn. Magn. Mater.* **200** 405
[16] Fernández I, Martín-González M S, Gonzalez-Arrabal R, Álvarez R, Briones F and Costa-Krämer J L 2008 *J. Magn. Magn. Mater.* **320** 68
[17] Shrestha S K, Timmers H, Butcher K S A S and Wintrebert-Fouquet M 2004 *Curr. Appl. Phys.* A **4** 237
[18] Terada S, Tanaka H and Kubota K 1989 *J. Cryst. Growth* **94** 567
[19] Wang D Y, Nakamine N and Hayashi Y 1998 *J. Vac. Sci. Technol.* A **16** 2084
[20] Pierson J F 2002 *Vacuum* **66** 59
[21] Kim K J, Kim J H and Kang J H 2001 *J. Cryst. Growth* **222** 767
[22] Ji A L, Huang R, Du Y, Li C R, Wang Y Q and Cao Z X 2006 *J. Cryst. Growth* **95** 79
[23] Hahn U and Weber W 1996 *Phys. Rev.* B **53** 12684
[24] Borsa D M and Boerma D O 2004 *Surf. Sci.* **548** 95
[25] Wang J, Chen J T, Yuan X M, Wu Z G, Miao B B and Yan P X 2006 *J. Cryst. Growth* **286** 407
[26] Liu Q Z, Yu L S, Deng F, Lau S S, Chen J W, Yang J W and Khan M A 1997 *Appl. Phys. Lett.* **71** 1658
[27] Liu Q Z and Lau S S 1998 *Solid State Electron.* **42** 677
[28] Dimitriadis C A, Karakostas Th, Logothetidis S, Kamarinos G, Brini J and Nouet G 1999 *Solid State Electron.* **43** 1969

[29] Liu Z Q, Wang W J, Wang T M, Chao S and Zheng S K 1998 *Thin Solid Films* **325** 55
[30] Ji Z, Zhang Y, Yuan Y and Wang C 2006 *Mater. Lett.* **60** 3758
[31] Mous D J W, Gottdang A and Haitsma R G 2001 *Nucl. Instrum. Methods* B **109** 177
[32] Mous D J W, Gottdang A, Haitsma R G, García-López G, Climent-Font A, Agulló-López F and Boerma D O 2003 *Instrum. Phys. CP* **680** 999
[33] Tesmer J R and Nastasi M 1995 *Handbook of Modern Ion Beam Materials Analysis* (Pittsburgh, PA: MRS) p 158
[34] Andrzejewska E, Gonzalez-Arrabal R, Borsa D and Boerma D O 2006 *Nucl. Instrum. Methods* B **249** 935
[35] http://www.LOT-Oriel.com
[36] Hou Z H 2008 *Solid State Sci.* **10** 1651
[37] Hoffman D W and Thornton J A 1976 *Thin Solid Films* **40** 355
[38] Hoffman D W and Gaerttner M R 1980 *J. Vac. Sci. Technol.* **17** 425
[39] Fox M 2001 *Optical Properties of Solids* (Oxford: Oxford University Press)
[40] Yue G H, Liu J Z, Li M, Yuan X M, Yan P X and Liu J L 2005 *Phys. Status Solidi* a **202** 1987